

Crystal growth of low dimensional spin systems

A. V. Prokofiev and W. Assmus*

Physikalisches Institut, J.W.Goethe Universität, Robert-Mayer-Str. 2-4, 60054 Frankfurt a.M., Germany

Crystal growth of the quasi-low dimensional spin systems $(VO)_2P_2O_7$, $LiCuVO_4$, $\alpha-CuV_2O_6$ and $CuSb_2O_6$ is reported. All substances are characterized by different kinds of instabilities. Vanadyl pyrophosphate either oxidizes in air or reduces in an inert atmosphere. It can be grown, however, from the melt in a special atmosphere, containing 0.1-0.7 mol.% of oxygen. The other compounds decompose before melting inevitably. Therefore techniques allowing growth at lower temperature were applied. Crystals of $LiCuVO_4$ and $\alpha-CuV_2O_6$ were grown from a flux. Corresponding phase diagrams solute-solvent were determined. For growth of $CuSb_2O_6$ crystals a chemical vapour transport technique was developed. The chemical processes in the gaseous phase were analyzed using thermodynamical calculations. The grown crystals were characterized by X-ray diffractometry and scanning electron microscopy with energy/wavelength dispersive X-ray analysis.

Key words: melt growth, flux growth, chemical vapor transport, low dimensional spin systems, phase diagrams.

Introduction

Low dimensional quantum spin systems are of fundamental interest due to their peculiar magnetic properties and their relevance to the problem of high- T_c superconductivity. Due to the important role of quantum fluctuations the quantum effects are more pronounced than in systems of higher dimensionality. One dimensional spin systems are more accessible to theoretical analysis. New real systems should serve for experimental tests of theoretical models. The most intensively studied materials are spin chain and spin ladder systems. All the spin chain systems display short range antiferromagnetic (AF) correlations at high temperatures. At lower temperature two different behaviors are possible. In most cases the systems undergo a transition to the 3D ordered state. However, very rarely a spin-Peierls transition may take place. Compounds of Cu^{+2} and V^{+4} attracted much interest as possible candidates for $S=1/2$ Heisenberg antiferromagnetic (AF) quantum spin chain and ladder systems. This paper is concerned with crystal growth of some compounds of this class.

As a catalyst vanadyl pyrophosphate (VOPO) has been widely investigated over the last decades. Due to its structure [1, 2] it attracted also the attention of physicists as a realisation of a spin-1/2 ladder system. Measurements made on powder materials were not able to answer the question which model fits better for VOPO-spin ladder or alternating spin chain. Therefore the interpretation of the magnetic properties has been revised several times [3, 4]. Only when the first single

crystals appeared it became possible to make neutron scattering experiments which determined unequivocally, that VOPO is an alternating spin chain system with the chains running along the [010] direction [5]. Later, on the basis of a monoclinic structure [2], it was found that two crystallographically slightly different types of VO chains exist in VOPO prepared at ambient pressure [6, 7].

$LiCuVO_4$ and $\alpha-CuV_2O_6$ contain in their structure crystallographic one-dimensional chains of edge-shared Cu-octahedra which are separated either by vanadium tetrahedra (in $\alpha-CuV_2O_6$) or both vanadium tetrahedra and lithium octahedra (in $LiCuVO_4$) [8, 9]. Magnetic measurements confirm that the two compounds are uniform spin chain systems. Both systems undergo an antiferromagnetic phase transition, at 2.6K in $LiCuVO_4$ and at 24K in CuV_2O_6 [10, 11, 12, 13]. Neutron scattering experiment showed that despite earlier expectations the spin chains in $\alpha-CuV_2O_6$ run not along the direction of the crystallographical chains of Cu-octahedra [010], but in the [110] direction because of a stronger next nearest neighbour coupling than the nearest neighbour one [14].

At room temperature $CuSb_2O_6$ has a monoclinically distorted trirutile type structure with the space group $P2_1/n$ [15]. A transition to the tetragonal trirutile type structure occurs above room temperature [16, 17]. Due to a strong anisotropy of the superexchange interaction in the nearly square Cu-sublattice monoclinic $CuSb_2O_6$ was reported to be a good realization of the one dimensional (1D) AF system [15]. At 8.6K a phase transition takes place which is displayed as a sharp anomaly in the temperature dependence of the magnetic susceptibility and in the heat capacity. Based on neutron powder diffraction investigations and the spin-flop transition observed in the magnetization measurements

*Corresponding author:
Tel : +49-69-798-23144
Fax: +49-69-798-28-520
E-mail: assmus@physik.uni-frankfurt.de

[18] this transition was assigned to 3D AF ordering. On the other hand in a recent study the temperature dependence of the nuclear spin-lattice relaxation rate shows an opening of a spin gap below 8.6K [19]. The authors have suggested that the transition in CuSb_2O_6 is of the spin-Peierls type.

Vanadyl pyrophosphate $(\text{VO})_2\text{P}_2\text{O}_7$

The heating of $(\text{VO})_2\text{P}_2\text{O}_7$ (VOPO) above 800°C in an inert atmosphere (or even at a lower temperature in vacuum) leads to the reduction of VOPO with the formation of a trivalent VPO_4 phase. On the other hand, at $500\text{--}600^\circ\text{C}$ in air VOPO oxidizes to the pentavalent VOPO_4 compound. Hence some intermediate conditions should be found to prevent VOPO from oxidation or reduction. It was found that VOPO is stable in oxygen concentrations of 0.1-0.7 vol.% and can be molten without decomposition.

However, the solidification of VOPO upon cooling results in the formation of glass instead of crystals because of the high viscosity of the VOPO melt [20]. Crystal growth from viscous melts has its own specificity. The growth rate should be very low.

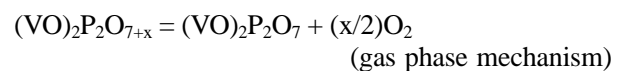
The scheme of the growth system is given in Fig. 1. We used a combination of Czochralski and Kyropoulos techniques, i.e. the cooling of the melt with simultaneous pulling of the grown crystals from the melt. Typical conditions were a cooling rate of 4-8 K/day and a pulling rate of 2-2.5 mm/day. The growth chamber was filled with a mixture of argon and a stabilized concentration of oxygen. In different runs we varied the

oxygen concentration in the range 0.1-0.7 vol.%. A platinum crucible was used.

Single crystals of a size up to $10 \times 5 \times 3 \text{ mm}^3$ were grown (Fig. 2a) [20]. According to the low temperature magnetic susceptibility measurements which are characteristic for the presence of any paramagnetic impurities or defects the grown crystals were of high quality [21]. X-ray powder diffraction and Laue pictures supported the idea of good crystal quality. However, the growth of VOPO is complicated by the following problem. Some of the crystals were transparent and firm, with mirror facets. However, some of the larger crystals, being perfect in appearance and having shining facets, were brittle and opaque in depth. According to X-ray diffraction the crystals of both types were single phase. They did not differ in quality according to the Laue pictures. The larger crystals gradually formed cracks and gradually broke into small pieces. Some inclusions of an amorphous second phase of a yellow color could be seen on the crack surfaces of the remaining pieces. These inclusions induced stresses in the crystals that led to the crack formation.

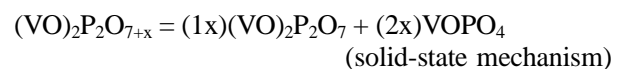
Based on a detailed differential thermal analysis (DTA) and thermo-gravimetric analysis (TGA) investigations of the interaction of VOPO with oxygen and other properties we came to the conclusion that a non-stoichiometric phase $(\text{VO})_2\text{P}_2\text{O}_{7+x}$ forms at temperatures close to the melting point of vanadyl pyrophosphate [22]. This phase is unstable at lower temperatures and decomposes in the stoichiometric compound $(\text{VO})_2\text{P}_2\text{O}_7$, losing oxygen.

There are two possible ways for the phase to become rid of excess oxygen. The first is the evolution of the gaseous oxygen:



The appropriate conditions for its realization exist only in the surface layer of the crystal, and it is this part of the crystal where it occurs. The mechanism preserves the surface layer of the crystal from inclusions of the VOPO_4 phase.

The second possibility, which can be realized only below 750°C , is a decay to two solid phases, one of them having a higher oxygen content than the other (disproportion):



As mentioned above, we found admixtures of a yellow VOPO_4 phase after the growth of our crystals.

Taking into account the size of our crystals, oxygen cannot travel a distance of several mm from the bulk to reach the surface. Therefore, the solid-state mechanism takes place in the inner part of the larger crystals.

This explains the better quality of the small crystals in comparison with larger ones.

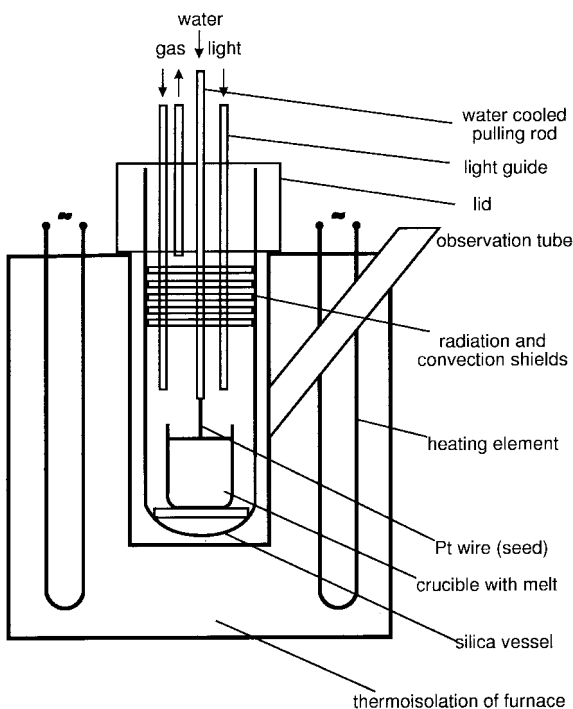


Fig. 1. Scheme of the growth system for vanadyl pyrophosphate.

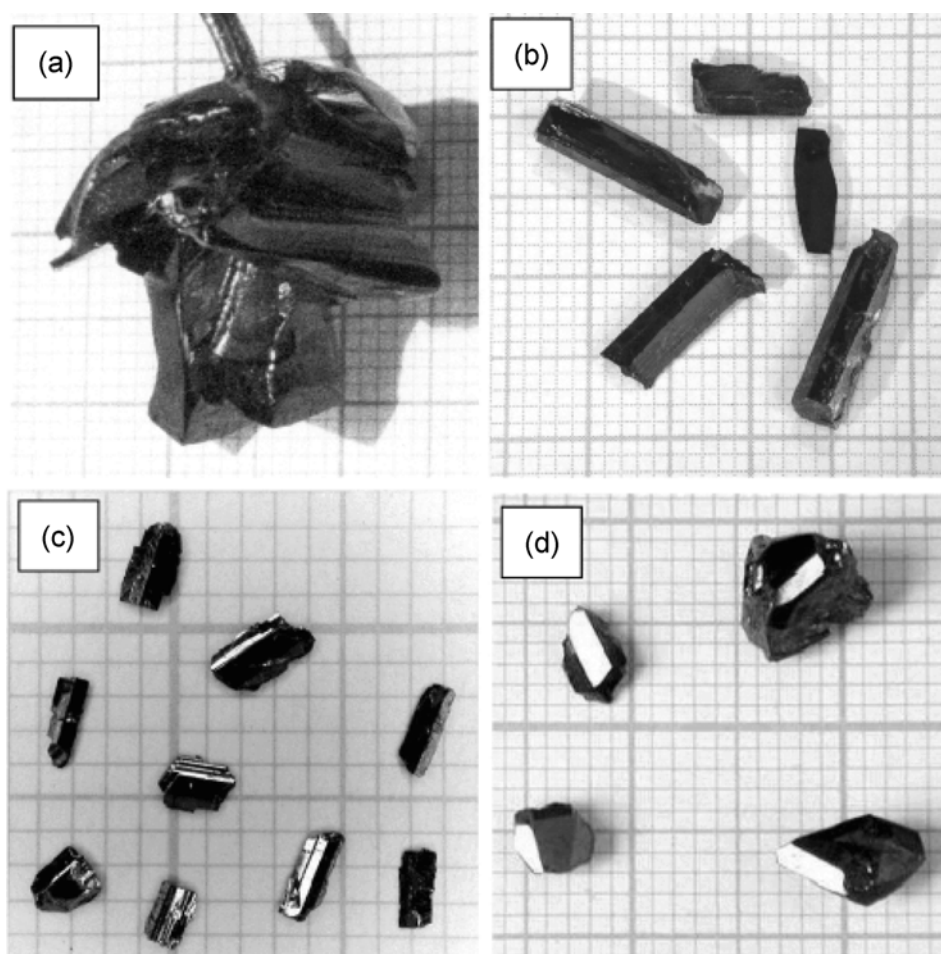
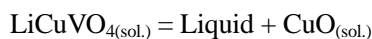


Fig. 2. Grown single crystals of low dimensional spin compounds (on a millimetre paper): (a) $(\text{VO})_2\text{P}_2\text{O}_7$; (b) LiCuVO_4 ; (c) $\alpha\text{-CuV}_2\text{O}_6$; (d) CuSb_2O_6 .

Crystals of the low pressure phase can be transformed by high pressure into the high pressure phase [23].

Lithium copper vanadate LiCuVO_4

LiCuVO_4 is a thermally unstable compound. DTA measurements and high temperature X-ray diffraction shows that at 640°C a peritectic reaction



takes place. Hence the crystals should be grown below this temperature. One of the ways to do this is by a solution growth method. As a “constituting part” of LiCuVO_4 the compound LiVO_3 may serve as a solvent. The $\text{LiCuVO}_4\text{-LiVO}_3$ diagram was investigated by DTA and high temperature XRD techniques, and the results are given in Fig. 3.

High temperature X-ray diffraction shows that there are no intermediate compounds between LiCuVO_4 and LiVO_3 . The eutectic composition was established to be 10 mole per cent LiCuVO_4 and 90 mole per cent LiVO_3 which melts at 550°C .

It is seen from the diagram that for compositions

between 10-60 mole% of LiCuVO_4 the melt co-exists only with the LiCuVO_4 solid phase. This field gives the most favourable conditions for the growth of LiCuVO_4 single crystals from solution in the LiVO_3 melt. The mixture with a composition of 40 molar per cent of LiCuVO_4 was held at 675°C and then cooled to 580°C with a cooling rate of 0.9 Kh^{-1} . This experiment yielded crystals with dimensions up to $12 \times 3 \times 3 \text{ mm}^3$ (Fig. 2b).

In our work we used LiVO_3 not only in a pure form but also in a mixture with LiCl . The eutectic composition 47 mol.% LiCl has the minimum melting point in the binary system $\text{LiVO}_3\text{-LiCl}$ [24]. The two variants (with LiVO_3 and the eutectics) have advantages and disadvantages. With the $\text{LiVO}_3\text{-LiCl}$ eutectic mixture as a solvent the crystallisation field is wider and one can choose a lower growth temperature, which results usually in crystals with lower concentrations of thermal defects. On the other hand the $\text{LiVO}_3\text{-LiCl}$ melt has a rather high LiCl vapour pressure above 500°C .

The phase diagram of the ternary $\text{LiCuVO}_4\text{-LiVO}_3\text{-LiCl}$ system was also investigated. The composition of this eutectics was evaluated to be about 7 mole per cent

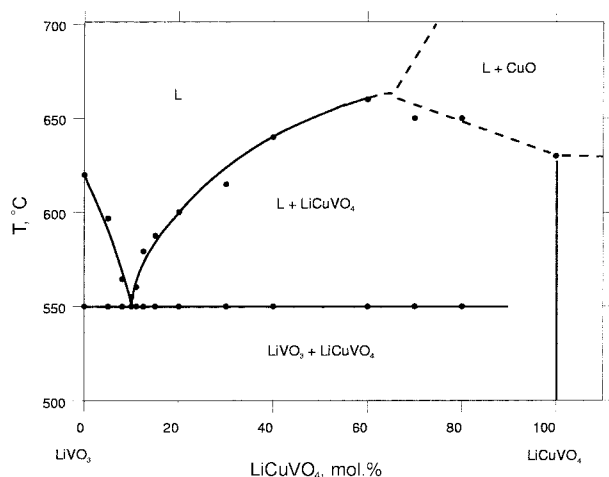


Fig. 3. Phase diagram of the quasi-binary system LiCuVO_4 - LiVO_3 .

of LiCuVO_4 . So, for the composition range 7-100% of LiCuVO_4 in a solution of the LiVO_3 - LiCl eutectics at temperatures higher than 460°C the liquid phase coexists with solid LiCuVO_4 .

Crystals with a maximum size of $1 \times 2 \times 4 \text{ mm}^3$ were grown from the LiVO_3 - LiCl melt [25]. Whereas the crystals grown at the same temperature in the LiVO_3 melt were tiny, the use of a LiVO_3 - LiCl solution allowed us to grow larger crystals even with a higher cooling rate.

The habit of the crystals varies. The most typical one is determined by the $\{001\}$, $\{021\}$, $\{101\}$, $\{201\}$ planes with a slight elongation of crystals in the $[100]$ direction. Lower temperature and cooling rates were found to facilitate a growth of needle-like crystals. The crystals are fragile and can be cleaved easily along the (001) planes forming mirror facets.

Copper divanadate CuV_2O_6

Like LiCuVO_4 , copper divanadate CuV_2O_6 is also thermally unstable and decomposes beginning at 635 - 640°C according to the peritectic reaction [26, 27]:



To find a relevant solvent for CuV_2O_6 we searched among the known phase diagrams for such a diagram where CuV_2O_6 is one of the components of a binary or a ternary oxide system [24]. The search led to Refs. 26 and 27. Despite some discrepancies above 640°C , one may conclude from both that CuV_2O_6 forms with V_2O_5 a solution of the eutectic type, the eutectic temperature being 620°C (see Fig. 4). The temperature interval of 620 - 640°C however is too small and the temperature is still too high to use V_2O_5 as a solvent for the growth of α - CuV_2O_6 (a phase transition to the β -modification takes place at 630°C [28]).

The melting temperature of the solution in V_2O_5 can be lowered, if a third component forming a eutectics

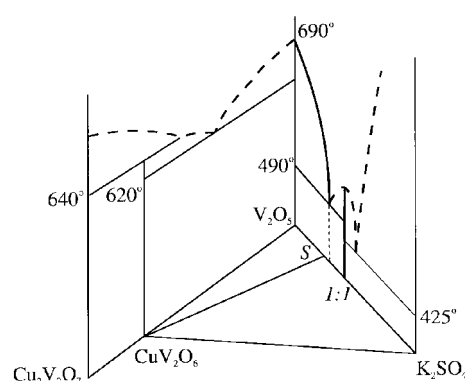


Fig. 4. Composition triangle of the CuV_2O_6 - V_2O_5 - K_2SO_4 phase diagram (the binary CuV_2O_6 - V_2O_5 and V_2O_5 - K_2SO_4 diagrams were taken from Ref. 24 and 26).

with V_2O_5 is added. In particular, the phase diagram V_2O_5 - K_2SO_4 determined in the early 1950s shows that potassium sulphate is appropriate for that [24] (see Fig. 4). The composition containing 65 mol.% V_2O_5 and 35 mol.% K_2SO_4 was reported to correspond to the eutectic point and to melt at 490°C . This mixture may be used as a solvent for the solution growth of CuV_2O_6 .

The phase diagram V_2O_5 - K_2SO_4 was reinvestigated in detail by DTA and it was concluded that a composition of 68 mol.% V_2O_5 and 32 mol.% K_2SO_4 (denoted further as S) seems to be optimal for the solvent [29].

After the selection of the optimal solvent we investigated the solubility of CuV_2O_6 in the solvent. In Fig. 4 the composition triangle of the CuV_2O_6 - V_2O_5 - K_2SO_4 ternary system is given. The phase diagram along the CuV_2O_6 -S line was the subject of our study.

The CuV_2O_6 -S pseudo-binary phase diagram was investigated by DTA and high temperature X-ray diffraction (HTXRD). The results are shown in Fig. 5 [29].

In the field of the CuV_2O_6 -S diagram between 10 and 80 mol.% CuV_2O_6 and between 478 and 630°C the CuV_2O_6 phase has been established to co-exist only

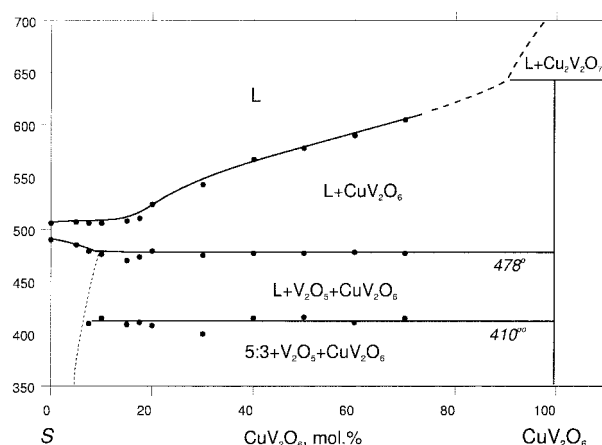


Fig. 5. Phase diagram CuV_2O_6 - solvent (68 mol.% V_2O_5 and 32 mol.% K_2SO_4).

with a liquid phase. This field gives the best conditions for growth of CuV_2O_6 crystals from solution in the $\text{V}_2\text{O}_5\text{-K}_2\text{SO}_4$ melt.

A slow cooling technique was used for the growth. The experiment was complicated by a strong tendency of the melt to creep over the crucible walls. This feature is characteristic for melts containing copper and vanadium (5+) oxides. We did not succeed in finding a crucible material which would solve this problem. This problem limited our abilities to achieve a large size of the crystals because of the relatively short growth time.

A mixture containing 60 mol.% of CuV_2O_6 and 40 mol.% of S was used to fill in an alumina crucible. The crucible was heated to 600°C , held 6 hour at this temperature and cooled down to 550°C over 20 hours.

After complete cooling the crucible was broken. The solidified mass contained crystals of CuV_2O_6 of a typical size of $2 \times 1 \times 0.5 \text{ mm}^3$ (Fig. 2c) [29]. We did not find a selective solvent for the isolation of the CuV_2O_6 crystals from the V_2O_5 -containing flux. However, cavities which were formed in the solidified melt, owing to the loss of the liquid phase, made it easy to isolate the crystals. Due to these cavities the single crystals appeared to be incompletely incorporated inside the melt, but partially free standing. This facilitated a mechanical separation of the crystals and partially saved their as-grown shiny facets.

EDX analysis of the CuV_2O_6 crystals shows that neither potassium nor sulfur contaminate the main phase within the sensitivity of the method of 0.1 at.%. Also, aluminum as a possible contamination from the crucible material was not found in the crystals.

Although X-ray powder diffraction shows that the crystals are single phase $\alpha\text{-CuV}_2\text{O}_6$ SEM/EDX analysis showed the presence of inclusions of foreign phases. Some of the crystal's surfaces contain inclusions of dimensions of $100 \times 100 \mu\text{m}$. The incorporated phases are V_2O_5 and an eutectic mixture of $\text{V}_2\text{O}_5\text{-}5\text{V}_2\text{O}_5 \cdot 3\text{K}_2\text{SO}_4$. A few per cent of aluminium was found to be incorporated in these inclusions.

Copper diantimonate CuSb_2O_6

Single crystals of CuSb_2O_6 have been grown earlier from a solution in a V_2O_5 melt [30, 31]. The crystals were of the size up to 2 mm. A contamination of the grown crystals by 2 wt.% and 0.48 wt.% [31] of vanadium was reported. The crystals were not characterized in detail by physical measurements. However such strong contaminations may be critical for the observation of a possible spin-Peierls transition in this compound which is usually very sensitive to impurities [32]. In order to obtain high purity crystals we applied a chemical transport technique. Earlier chemical transport experiments showed their effectiveness for growth of many complex oxides, particularly of tantalates and niobates with a similar

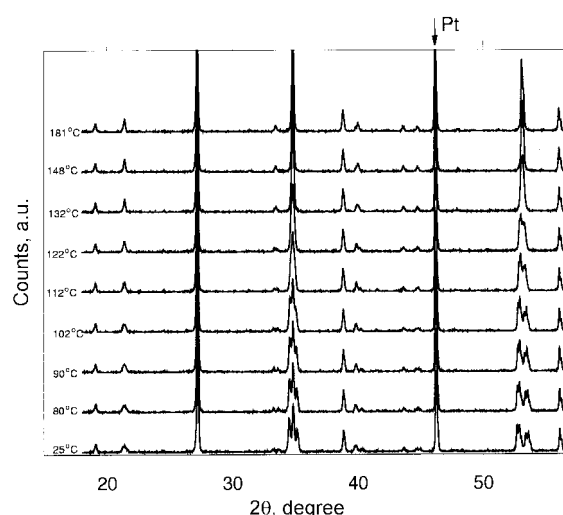


Fig. 6. In situ X-ray powder diffraction of CuSb_2O_6 in the temperature range of $25\text{-}168^\circ\text{C}$. The peak at $2\theta=47^\circ$ originates from the platinum heater. The monoclinic-to-tetragonal transformation, as e.g. the peak splitting at 35° shows, finishes at about 122°C .

formula MT_2O_6 and structure [33, 34].

DTA and TGA show that CuSb_2O_6 remains stable to heating in air up to about 1120°C . Starting from this temperature a strongly endothermic process accompanied by a sharp mass decrease of the crucible content occurs. CuSb_2O_6 decomposes at this temperature mainly according to the reaction



A tetragonal-to-monoclinic structural phase transition was variously reported to occur at 227°C [15] or 107°C [16]. In order to resolve this discrepancy the transition was investigated in the present work by in-situ high temperature X-ray diffraction and by DTA. The temperature evolution of the CuSb_2O_6 XRD pattern with characteristic transformation of the (hkl) , (khl) and $(\bar{h}kl)$ triple of the monoclinic phase into the (hkl) single peak of the tetragonal modification is presented in Fig. 6. The transformation, as e.g. the peak splitting at 35° shows, finishes at about 122°C . This agrees also with our DTA investigations. DTA heating and cooling curves are characterized by a broad anomaly corresponding to an extended reversible phase transition between 100°C and 130° (Fig. 7). Both measurements confirm the transition temperature reported by Gier *et al.* [17].

For selection of an appropriate transport agent and evaluation of the transport conditions, thermodynamic simulation of transport systems was carried out. For calculation of chemical equilibria a program for minimization of the free energy of the reaction system as a function of the mole fractions of the gaseous and solid components constrained by mass-balance conditions was used [35].

The chemical equilibria of CuSb_2O_6 with chlorine-containing compounds TeCl_4 , HCl and Cl_2 as candidates

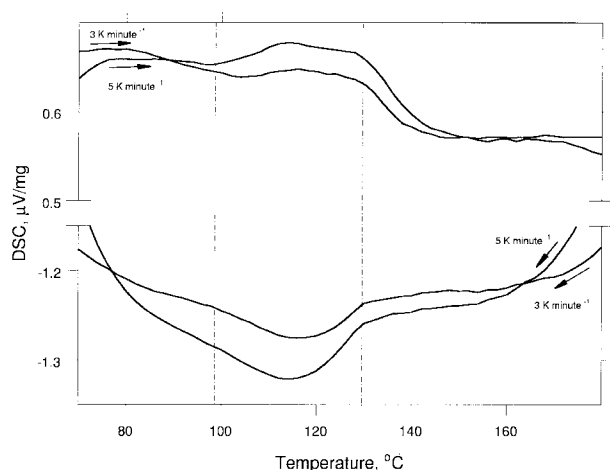


Fig. 7. DTA heating and cooling curves in the vicinity of the structural monoclinic-to-tetragonal phase transition of CuSb_2O_6 .

for transport agents in the temperature range of 750-1150°C were simulated. The calculations show, that for all transport systems the quantity of Cu and Sb in the gas phase rises monotonically with temperature. Therefore

copper antimonate is transported from the hot to the cold zone. Because of a relatively weak temperature dependence of the CuSb_2O_6 -HCl equilibrium, this systems seems the least favourable for transport. Moreover, introducing gaseous HCl into the ampoule is difficult. Based on the simulation, the transport of CuSb_2O_6 with chlorine in the temperature range of 800-900°C and TeCl_4 in the temperature range of 870-1000°C were selected for our experimental investigations.

For these conditions chemical transport of CuSb_2O_6 was realized experimentally (chlorine was introduced in the ampoule as CuCl_2 which gives on decomposition chlorine and gaseous CuCl). Well faceted crystals have been grown with both transport agents at the cool end of the ampoule, in accordance with the calculations. Transport with TeCl_4 results in a higher transport rate and bigger crystals of a size up to 125 mm^3 [36] (Fig. 2d). In the case of the Cl_2 -transport a substantial amount of CuCl as a secondary product of the decomposition of CuCl_2 is formed in the gaseous phase. This results in a higher total pressure and therefore in a lower diffusion rate of the components in the ampoule.

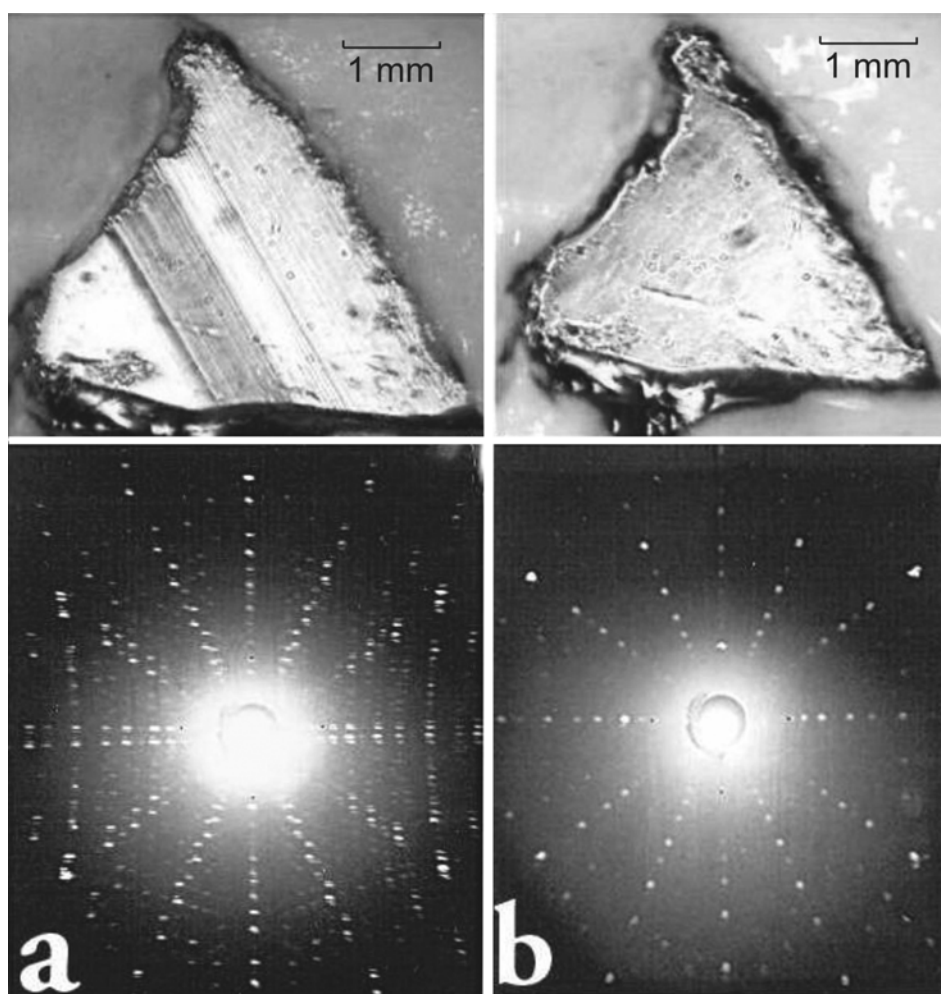


Fig. 8. Stripes on the CuSb_2O_6 crystal's surface, their disappearance at the phase transition and the corresponding Laue photographs; a) at 25°C (monoclinic), b) at 150°C (tetragonal).

X-ray diffraction of powdered crystals shows the absence of any foreign phases. Rietveld refinement of the diffraction pattern gives the cell values $a = 4.6362 \text{ \AA}$, $b = 4.63710.0 \text{ \AA}$, $c = 9.29900.0 \text{ \AA}$, and $\beta = 91.099^\circ$.

SEM observation of polished surfaces of cut crystals and growth facets also did not reveal any inclusions of foreign phases. EDX/WDX analysis detects neither tellurium nor chlorine contaminations in the CuSb_2O_6 crystals grown with TeCl_4 (the sensitivity of WDX is about 0.1 at.%). Silicon, a possible contamination from the reactor walls, was also not evident in the crystals.

Two types of twinning were observed in the crystals grown in the present work: growth twinning (which takes place in the tetragonal phase at the growth temperature of 800-900°C) and multiple twinning due to the structural phase transition which occurs at 110°C during the cooling of the crystals to room temperature. The formation of the growth twins was observed for the majority of the grown crystals. The boundary between two twins can be seen clearly under a polarized light microscope. The contact twins composing the grown bi-crystals (or sometimes tri-crystals) were separated by cutting along the composition plane. Laue tests of several twins always showed that the composition planes are the {013} twin planes, which are the mirror planes in the tetragonal CuSb_2O_6 growth twin.

A more serious problem is the twinning due to the structural phase transition. An investigation with normal and polarized optical microscopy reveals that the as-grown shiny surfaces of the crystals have a typical twin microstripe pattern. In Fig. 8a (upper) an as-grown (100) facet of a crystal is shown. The fine stripes are distributed not equally over the surface. There are regions on the surface with higher and lower density of stripes, as well as regions without them at all. The stripes disappear above 110°C (Fig. 8b, upper), proving their twin origin. In the bottom part of the figure the corresponding Laue photographs taken on the same point of the surface of the crystal below and above the structural transition temperature are shown.

We tried to detwin the crystals by application of a uniaxial pressure. A thermal treatment under a uniaxial pressure of 30 MPa was performed normal to the (101) surface. Two regimes of temperature treatment were used: annealing below the transition at 50-100°C and slow cooling from 130°C through the phase transition down to 80°C. The crystals were checked after the treatment for peak splitting with the X-ray counter diffractometer. No sign of detwinning was observed. Further increase of the load was hardly possible because of the limit of mechanical stability of the crystals. The same procedure was applied, also unsuccessfully, to other crystals with pressure along the $[\bar{1}03]$ and $[100]$ crystal axes.

The main goal of developing crystal growth was further physical investigations of the crystals. All crystals were therefore characterized by measurements of the magnetic susceptibility, specific heat and other

properties. For this information we refer the reader to Ref. 21, 22, 25, 29, 36.

Acknowledgement

The work was supported financially within the DFG Schwerpunktprogramm 1073 "Kollektive Quantenzustände in elektronisch eindimensionalen Übergangmetallverbindungen".

References

1. Y.E. Gorbunova, S.A. Linde. Doklady Akad. Nauk SSSR. 245 (1979) 584-588.
2. P.T. Nguyen, R.D. Hoffman, A.W. Sleight. Mater Res Bull 30 (1995) 1055-1063.
3. D.C. Johnston, J.W. Johnson, D.P. Goshorn, and A.J. Jacobson. Phys. Rev. B365 (1987) 219-222.
4. T. Barnes, J. Riera. Phys. Rev. B 50 (1994) 6817-6822.
5. A.W. Garret, S.E. Nagler, D.A. Tennant, B.C. Sales, and T. Barnes. Phys. Rev. Lett 79 (1997) 745-748.
6. Z. Hiroi, M. Azuma, Y. Fujishiro, T. Saito, and M. Takano. J. Solid State Chem. 146 (1999) 369-379.
7. J. Kikuchi, K. Motoya, T. Yamauchi, and Y. Ueda. Phys. Rev. B 60 (1999) 6731-6739.
8. M.A. Lafontaine, M. Leblanc, and G. Ferey. Acta Crystallographica, C45 (1989) 1205-1206.
9. C. Calvo and D. Manolescu. Acta Cryst. B29 (1973) 1743-1745.
10. M. Yamaguchi, T. Furuta, and M. Ishikawa. J. Phys. Soc. Japan. 65 (1996) 2998-3006.
11. A.N. Vasil'ev. JETP Lett. 69 (1999) 876-880.
12. A.N. Vasil'ev, L.A. Ponomarenko, A.I. Smirnov, E.V. Antipov, Yu.A. Velikodny, M. Isobe, and Y. Ueda. Phys. Rev. B60 (1999) 3021-3024.
13. A.N. Vasil'ev, L.A. Ponomarenko, E.V. Antipov, Yu.A. Velikodny, A.I. Smirnov, M. Isobe, and Y. Ueda. Physica B 284-288 (2000) 1619-1620.
14. J. Kikuchi, K. Ishiguchi, K. Motoya, M. Itoh, K. Inari, N. Eguchi, and J. Akimitsu. J. Phys. Soc. Jpn. 69 (2000) 2660-2668.
15. A. Nakua, H. Yun, J.N. Reimers, J.E. Greedan, and C.V. Satger. J. Sol. State Chem. 91 (1991) 105-112.
16. J.D. Donaldson, A. Kjekshus, D.G. Nicholson, and T. Ranke. Acta Chem. Scand. Ser. A 29 (1975) 803-807.
17. O.-E. Gieré, A. Brahimí, H.J. Deiseroth, and D. Reinen. J. Sol. State Chem. 131 (1997) 263-274.
18. A.M. Nakua and J.E. Greedan. J. Sol. State Chem. 118 (1995) 199-201.
19. M. Kato, A. Hatazaki, K. Yoshimura, and K. Kosuge. Physica B, 281&282 (2000) 663-664.
20. A.V. Prokofiev, F. Büllersfeld, and W. Assmus. Cryst Res Technol 33 (1998) 157-163.
21. A.V. Prokofiev, F. Büllersfeld, W. Assmus, H. Schwenk, D. Wichert, U. Löw, and B. Lüthi. Eur. Phys. J B5 (1998) 313-316.
22. A.V. Prokofiev, F. Büllersfeld, and W. Assmus. Mater. Res. Bull. 35 (2000) 1859-1868.
23. C. Gross, M. Anton, A. Löffert, A. Prokofiev, and W. Assmus. High Press. Res. 22 (2002) 581-584.
24. Phase Diagrams for Ceramists. Ed. by M. Ernest, R. Carl and H.F. McMurdie. 1964-1983, V. 1-5.
25. A.V. Prokofiev, D. Wichert, and W. Assmus. J. Cryst.

- Growth. 220 (2000) 345-350.
26. V. Cirilli, A. Burdese, and C. Bristi. *Atti. Accad. Sci. Torino*, 95 (1961) 15-20.
 27. P. Fleury. *C.R. Acad. Sci., Ser. C* 263 (1966) 1375-1380.
 28. D. Mercurio *et al.* *C. R. Seances Acad. Sci., Ser. C*282 (1976) 27-31.
 29. A.V. Prokofiev, R.K. Kremer, and W. Assmus. *J. Cryst. Growth*. 231 (2001) 498-505.
 30. S. Shimara, K. Kodaira, and T. Matsushita. *J. Cryst. Growth*. 72 (1985) 753-755.
 31. A.M. Nakua and J.E. Greedan. *J. Cryst. Growth*. 154 (1995) 334-338.
 32. R. Melin. *Eur. Phys. J. B* 16 (2000) 261-268 and references therein.
 33. R.K. Kremer and J.E. Greedan. *J. Sol. State Chem.* 73 (1988) 579-582.
 34. R.K. Kremer, J.E. Greedan, E. Gmelin, W. Dai, S.M. Eicher, and K.J. Lushington. *J. de Physique. Colloq.* C8 49 (1989) 1495-1502.
 35. A.V. Golubkov and A.V. Prokofiev. *Russ. J. Inorg. Mater.* 27(2) (1991) 234-238.
 36. A.V. Prokofiev, F. Ritter, W. Assmus, B.G. Gibson, and R.K. Kremer. *J. Cryst. Growth* 247 (2003) 457-466.